Theoretical and Experimental Investigation of a Rectenna Element for Microwave Power Transmission

James O. McSpadden, Taewhan Yoo, and Kai Chang, *Fellow, IEEE*

***Abstract*—The diode characteristics at 2.45 and 35 GHz and the use of a frequency selective surface are investigated for the application of microwave power transmission. A method has been devised to experimentally characterize a packaged GaAs Schottky barrier diode by inserting in a microstrip test mount. The nonlinear equivalent circuit parameters of the diode are determined by a small signal test method. The method analyzes the diode's scattering parameters at various bias levels. A large signal measurement using the same test mount has also been configured to determine the power conversion efficiency from microwave to dc as well as determining the de-embedded network impedance of the diode. A nonlinear circuit simulation program using a multi-reflection algorithm is used to verify the experimental results of a 2.45 GHz diode. A *Ka*-band mixer diode is also simulated for a 35 GHz rectenna. Based on the simulation results, a patch-type 35 GHz rectenna is designed and tested in a waveguide simulator. The efficiency is measured as 29% with a 120 mW input power. Because the diode could generate undesirable harmonic radiation, a frequency selective surface is designed to reduce the second harmonic radiation for a 2.45 GHz rectenna. Theoretical results agree fairly well with experiments for all these studies.**

I. Introduction

The RECEIVING rectifying antenna (rectenna) is one of the main components of microwave power transmission systems. In order for such systems to operate cost-efficiently in land or spaced-based locations, the conversion efficiency from microwave to dc of the rectenna must be high. Rectannas were first practically designed in the early 1960's for 2.45 GHz operation [1]. Since that time, the conversion efficiencies have been improved from 38% to over 85% [2]–[4]. The main reason for the rise in the efficiency was the improvement in the diode and circuit construction for high input power levels [5].

The GaAs diode which rectifies the received incident power has been analyzed at small and large signals in a microstrip test mount at 2.45 GHz [6]. Previous work has been published on a microstrip test mount where the diode was shunted to the ground plane at the end of an open-ended microstrip line [7]. The microstrip test mount presented in this paper is a 2-port device which allows the measurement of the four scattering parameters. The diode is tested at small signal levels for determining the circuit model and tested at large signal levels for determining the microwave to dc power conversion efficiency as well as the diode input impedance.

For microwave power transmission, the diode conversion efficiency is a key element for implementing successful systems [1]. The rectenna incorporates this type of GaAs Schottky barrier diode to convert the received beam into useful dc power. Computer programs can be used to predict rectenna performance by including accurate diode parameters. The ability to experimentally characterize the diode operating under high power conditions enables efficient design of the rectenna circuitry. The microstrip test mount allows the diode to be measured in both small and large signal conditions. Measured and theoretical results are presented for the method of matching the circuit to the diode.

The multi-reflection algorithm which was originally developed by Held and Kerr for the analysis of mixers [8] is used to simulate the rectenna circuit. The efficiency of a 2.45 GHz rectenna is simulated using the diode equivalent circuit obtained from the small signal test results. The calculated and measured conversion efficiencies are compared. The program is also used to predict the efficiency of a 35 GHz rectenna using an equivalent circuit of a *Ka*-band mixer diode provided by the manufacturer. A 35 GHz rectenna is designed with a microstrip patch antenna and the mixer diode [9]. The rectenna is tested in a waveguide simulator.

One of the main problems of a rectenna array is the harmonic radiation generated by the diode that performs the rectification. For efficient conversion the harmonic energy is generally trapped near the diode by low pass filters. However, a small but finite value of harmonic energy is reradiated [10]. In an attempt to suppress the second harmonic radiation, a novel idea of using a frequency selective surface (FSS) has been designed to pass the fundamental frequency of 2.45 GHz and block the second harmonic of 4.9 GHz [11]. The FSS is placed in front of the rectenna array $\lambda/4$. The FSS could also act as a shield to protect the rectenna circuitry from the adverse environment. The rectenna system that includes the

Manuscript received March 31, 1992; revised July 27, 1992. This work was supported in part by the NASA Center for Space Power at Texas A&M and the Army Research Office.
The authors are with the Department of Electrical Engineering, Texas A&M University, College Station, TX 77843.
IEEE Log Number 9203695.

FSS, rectenna plane, and reflecting plane is shown in Fig. 1.

II. Small Signal and Large Signal Diode Characterization at 2.45 GHz

A. Test Mount Design

A microstrip test mount is designed and constructed for small signal and large signal operation. The height of the ceramic or glass wall on the screw-type diode determines the appropriate thickness of substrate to use. The Through-Reflect-Line (TRL) calibration used by the HP8510B network analyzer is required for proper calibration. As shown in Fig. 2, a 50 Ω microstrip line has a hole drilled at the center of the board. The diameter of the hole is the same diameter of the diode. The quasi-TEM reference plane is located at the center of this hole. Due to the large height of the diode ceramic wall, the substrate is made of 60 mil RT/duroid with a dielectric constant of 2.2. Open, through the delay boards as shown in Fig. 3 were constructed for the TRL calibration using the same type of substrate.

B. Small and Large Signal Measurement Setup

The experimental setup for the small signal testing is shown in Fig. 4. Bias tees are added to provide different bias locations while measuring the scattering parameters and to provide dc signal isolation from the HP8510B. Due to the frequency restriction of TRL calibration, the testing frequencies ranged from 600 MHz to 4.2 GHz.

The large signal test setup is shown in Fig. 5. The input and reflected power on the source side of the mount are measured to determine the overall input power. A low pass filter is added to prevent the harmonics produced by the source from being measured as input power. The double stub tuners are used to maximize the output dc power. Bias tees are also added to the setup for measuring the dc voltage across a known resistive load and to provide dc isolation from the rest of the setup. A short is placed at the end to reflect the microwave power. After achieving over 70% conversion efficiency, the bias tees and tuning stubs are removed from the large signal test setup and connected separately to the setup as shown in Fig. 6. The setup in Fig. 6 is calibrated by the TRL method which locates the reference plane at the center of the through board where the diode would be located. Because the frequency span does not cover the higher order harmonic frequencies, a second calibration technique is employed for measuring the scattering parameters from 2 to 8 GHz. Port 1 of the HP8510B is calibrated by open, short, and load terminations. The impedance measured is modified by an extra delay from the calibrated reference plane to the end of the open microstrip board. The end of the open microstrip board is the location of the diode center.

C. Small and Large Signal Measurement

For the small signal testing of the GaAs Schottky diode, the scattering parameters for the frequency range (600

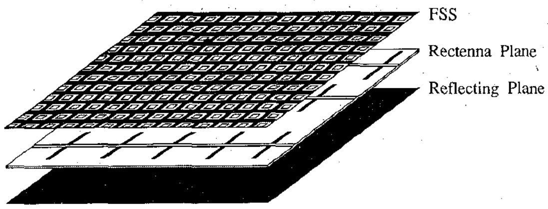

Fig. 1. Components of rectenna system including a frequency selective surface, rectenna plane, and reflecting plane.

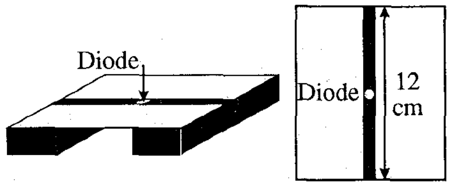

Fig. 2. Microstrip diode test mount.

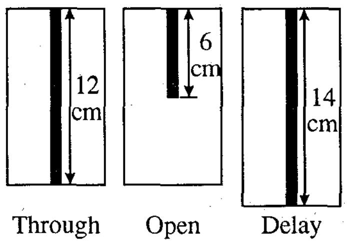

Fig. 3. Microstrip TRL calibration boards.

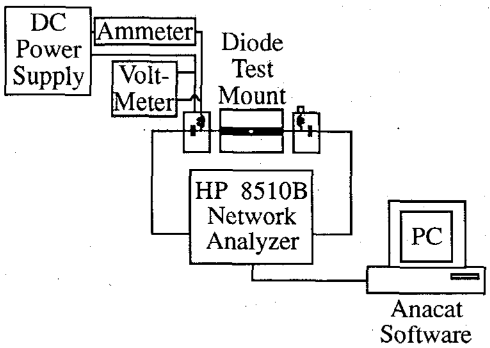

Fig. 4. Small signal test setup, 600 MHz–4.2 GHz.

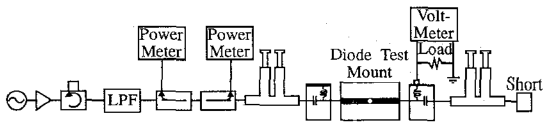

Fig. 5. Large signal test setup, 2.45 GHz.

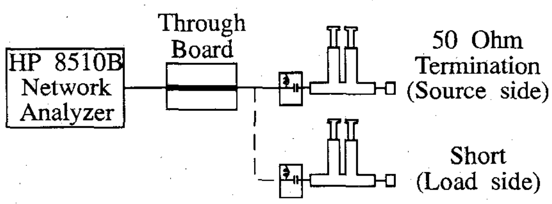

Fig. 6. Circuit impedance measurement as seen by the diode under large signal testing.

MHz–4.2 GHz) were measured at eight different bias levels (4 reverse bias, 1 zero bias, and 3 forward bias). The use of different bias voltages characterizes the nonlinear effect of the diode. Touchstone was then used to determine the diode circuit parameters by the optimize command that curve fits the diode circuit model to the measured scattering data. From the scattering parameter measurement and the Touchstone optimization, one can determine the lead inductance L_p, the package capacitance C_p, the series resistance R_s, the junction resistance $R_j(V)$, and the junction capacitance $C_j(V)$.

The small signal circuit results are shown in Figs. 7, 8, and 9. After the initial optimization by Touchstone of the eight scattering parameter files was completed, the assumed bias independent parameters (L_p, R_s, and C_p) were selected. These parameters were based on the optimized result and data given by the manufacturer [5], [12]. The nonlinear circuit model was solved as shown in Fig. 7. Using these bias independent parameter values, the bias dependent parameters (R_j and C_j) were found by running the optimization routine once more. Fig. 8 shows the *CV* characteristic curves from the calculated and measured data. The calculated curve is based on the equation given by the manufacturer for these particular diodes [12]:

$$C_j = C_o \sqrt{\frac{0.8}{0.8 - V}}$$

C_o is the zero bias junction capacitance (3.55 pF) and V is the bias voltage. Fig. 9 shows the measured junction resistance as a function of bias.

For the large signal testing, 1.2 W was used as the operating power level. The stub tuners maximized the output dc voltage or achieved over 70% conversion efficiency while also minimizing the reflected power. The tuners were then removed from the test setup shown in Fig. 5 and connected to the HP8510B as shown in Fig. 6. The input impedance of the tuners were measured separately by the HP8510B and the overall circuit impedance was found by adding the two measured values in parallel. The second harmonic circuit impedance at 4.9 GHz was also determined with the tuners by using the second calibration method mentioned previously.

A microwave to dc conversion efficiency of 85% has been achieved in our large signal test setup. The conversion efficiency was calculated by

$$\text{Conversion Efficiency} = \frac{\dfrac{V_{DC}^2}{R_{load}}}{P_{in} - P_{reflected}}$$

where the load was 202 Ω. A system error of 4% in the measured conversion efficiency is based on the variance of loss through the experimental setup (Fig. 5). The measured impedances at the fundamental and second harmonic frequencies at various efficiency locations are shown in Fig. 10. The various impedances at the fundamental frequency demonstrate a trend as the efficiency is increased. These points are the circuit impedances as seen

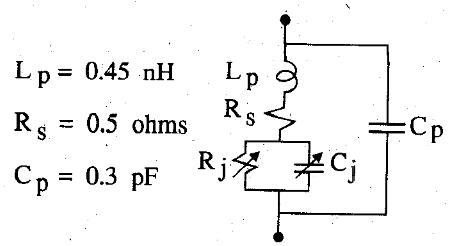

Fig. 7. Small signal equivalent circuit of GaAs diode and experimental values for parasitic elements.

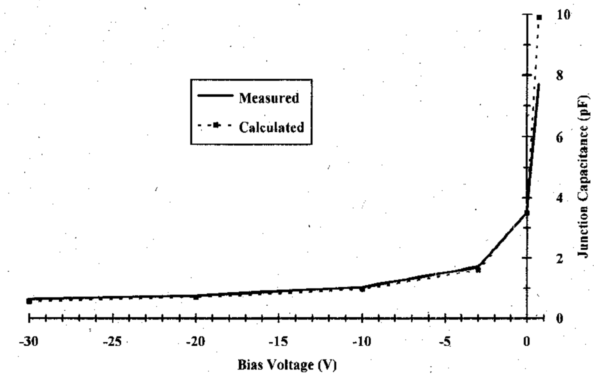

Fig. 8. Calculated and measured junction capacitance vs. bias voltage.

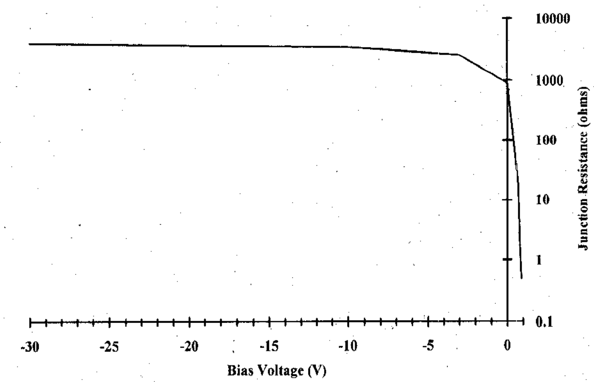

Fig. 9. Measured junction resistance versus bias voltage.

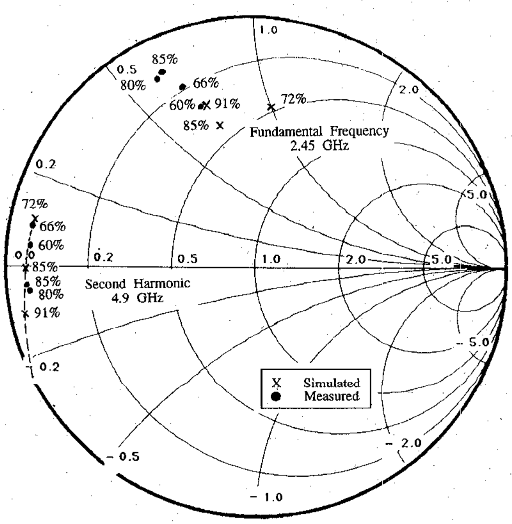

Fig. 10. Measured and theoretical circuit impedances as seen by the diode when operating under large signal condition at 2.45 and 4.9 GHz.

by the diode. Ten diodes were tested and the typical maximum conversion efficiency was 80%. The circuit impedance as seen by the diode was approximately 6 + j29 Ω at 2.45 GHz. By taking the complex conjugate, the diode input impedance is determined to be 6 − j29 Ω. A simple model of a resistor and capacitor connected in series is implied. The impedance is transformed into admittance as 0.00684 + j0.033 mhos. Taking the inverse of the real part, the resistance of the diode for matching purposes is 146 Ω. This value agrees well with experiments to determine the load impedance for the highest conversion efficiency. The load is typically 1.3 to 1.4 times the input resistance of the diode [13]. The second harmonic impedance points lie near the short position which is expected for diodes in an efficient rectenna.

Based on the trend of the impedances of the fundamental frequency and the approximate short location of the second harmonic impedances, this method appears sound for determining the input impedance of the Schottky barrier diode for the rectenna application.

III. Nonlinear Circuit Simulation of the 2.45 GHz Rectenna

A. Nonlinear Circuit Simulation Computer Analysis

The rectenna is a nonlinear circuit converting microwave power into dc power. The conversion efficiency and the impedance of the diode depend on the impedance condition at all the frequencies including dc. The rectenna circuit is simulated by the computer analysis that divides the circuit into linear and nonlinear networks. The nonlinear network contains the intrinsic diode consisting of the junction resistance and the junction capacitance. The linear network includes the diode parasitic elements and the linear circuit surrounding the diode. The voltage wave generated from one network propagates to the other network through an artificial transmission line. The artificial transmission line impedance was varied between 100 Ω and 200 Ω in order to determine the fastest convergence. The response of the intrinsic diode in the nonlinear network was calculated in the time domain and sampled at 256 points. An IMSL, Inc., subroutine called "IVPRK" was used for calculating the time domain response. A fast Fourier transform was used to transform the signal between the time domain and the frequency domain. The highest harmonic included in the calculation was the $128^{\text{th}} f_o$. The formula to calculate the convergence to the steady state solution is given as

$$\frac{\sum_{i=0}^{i=255} |\Delta V_i|}{256} \leq \text{MAX}(\text{Error}, \text{Error} \cdot |V_{\max}|)$$

where Error is 0.005. Because the linear circuit is defined in the frequency domain, the impedance of the different harmonics can be independently specified. Therefore, the conversion efficiency of the rectenna can be tested by specifying different circuit impedances.

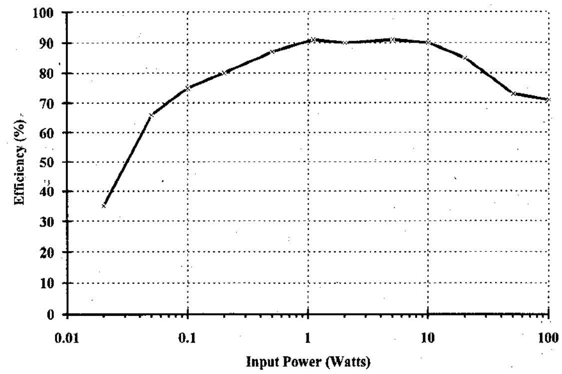

Fig. 11. Conversion efficiency vs. input power for 2.45 GHz rectenna.

B. Computer Simulation and Large Signal Measurement Comparison

The equivalent circuit of the diode in Fig. 7 was used in the computer simulation. The efficiencies calculated from the simulation were compared with the large signal test results. In the simulation, the dc load resistance and source power were set to be 200 Ω and 1.2 W. The efficiency was maximized when the linear circuit impedances of the higher order harmonics were set to zero at the junction terminals of the intrinsic diode. The maximum efficiency and the impedance of the packaged diode were calculated as 91% and 15 + j35 Ω, respectively. These calculated values are consistent with the measured values of 85% and 6 + j29 Ω.

The maximum simulated efficiency of 91% occurred when the second harmonic impedance of the packaged diode was set to −j13 Ω. In order to relate the simulated results to the large signal test results, the second harmonic impedances were varied between 4 + j5 Ω, and 2 − j5 Ω. The efficiency was maximized with these second harmonic impedances by varying the fundamental impedance. The simulated results are plotted as crosses on Fig. 10. As seen from the figure, the calculated conversion efficiency increased from 72% to 91% as the second harmonic impedance approaches −j13 Ω. The calculated efficiency follows the same trend of the measured efficiencies. The inconsistencies in the measured results with the simulated results can be related to the effect of the third and higher order harmonic impedances.

C. Variation of Maximum Efficiency with Power

The maximum efficiency of the 2.45 GHz rectenna was simulated with different power levels. The power was varied from 0.02 W to 100 W. The conversion efficiency was calculated for each power level by the simulation. The results are shown in Fig. 11. The efficiency was calculated to be over 90% in the power range between 1 and 10 W. The efficiency at 0.05 W was 66% and was 71% at 100 W. From this result, it can be concluded that the diode can work at a high conversion efficiency over a broad power range.

IV. A 35 GHz Rectenna

A. Nonlinear Simulation of a Ka-band Mixer Diode

A *Ka*-band mixer diode was used in the design of a 35 GHz rectenna. The efficiency and optimum fundamental frequency impedance of the diode were calculated by the simulation program. The equivalent circuit shown in Fig. 12(a) was obtained from the data sheet provided by the manufacturer. A resistive diode shown in Fig. 12(b) was realized by omitting all the reactive elements from the equivalent circuit. The resistive diode was used to investigate the effects of the reactive elements on the efficiency of the 35 GHz rectenna. Each point in Fig. 13 shows the power conversion efficiency calculated for the given dc load resistance and dc output power. The solid circles are the results calculated with the actual diode and the cross points are the results calculated with the resistive diode.

The efficiency of the resistive diode increases to 70% as the operating power level increases. The optimum dc resistance for the maximum efficiency increases as the power level decreases. In other words, the optimum dc load resistance is small for a high output power. This condition is a result of the limitation on the output dc voltage. The output dc voltage is limited below $\frac{1}{2}$ of the breakdown voltage V_{br}. A small dc load resistance should therefore produce the high power with the limited dc output voltage. At the low operating power region, the effective diode impedance of the resistive diode increases with increasing dc load resistance. Therefore, the effect of the series resistance of the diode becomes small compared to the diode impedance. This effect results in a small diode loss at the series resistor and a high conversion efficiency.

However, the impedance of an actual diode cannot be increased as that of the resistive diode. The junction capacitance of the actual diode limits the diode impedance. If the actual diode is forced to operate with a high impedance, a large current will flow through the junction capacitance. This current flow will result in a low power conversion efficiency. According to the calculated results shown in Fig. 13, the maximum efficiency of the actual diode follows the efficiency of the resistive diode in the high power region. This condition continues until the optimum dc load resistance reaches 100 Ω. The maximum efficiency becomes constant in the low power region. This constant efficiency occurs because the junction capacitance prevents the dc load resistance from increasing to more than 100 Ω. Therefore, the bend on the maximum efficiency curve seen in Fig. 13 offers the optimum design parameters for maximum conversion efficiency and output power. The optimum diode impedance, dc load resistance, and output power are found as 40 Ω, 100 Ω, and 30 mW, respectively. The second harmonic impedance is calculated as −j87 Ω. The maximum power conversion efficiency is then estimated to be approximately 50% with these design parameters when the net input power is 60 mW.

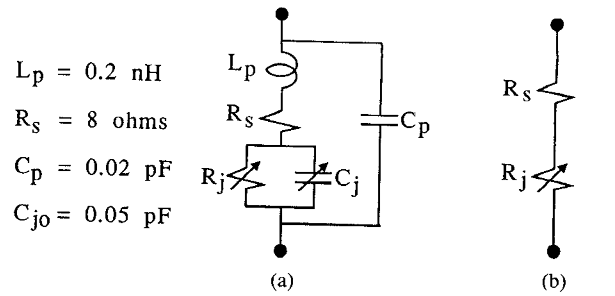

Fig. 12. (a) The equivalent circuit of a Schottky diode and (b) a resistive diode obtained by omitting the reactive elements of the circuit in (a).

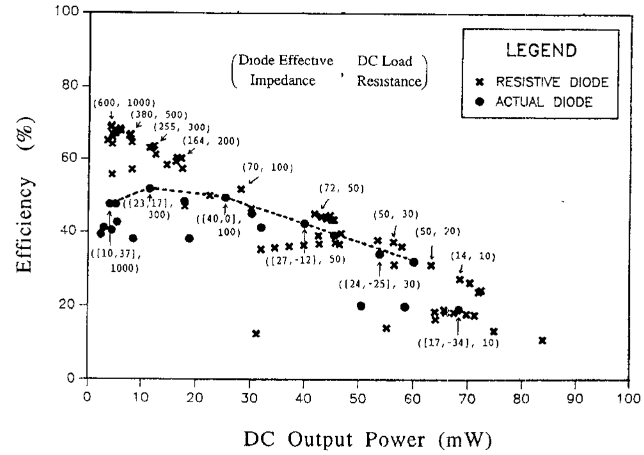

Fig. 13. The power conversion efficiency of a *Ka*-band mixer diode calculated with the multi-reflection method for various RF and dc impedances. The parameters of the GaAs Schottky diode are: $R_s = 8$ Ω, $V_{br} = 5$ V, $I_s = 0.037$ pA, $C_{jo} = 0.053$ pF, $\gamma = 0.5$, $L_p = 0.2$ nH, $C_p = 0.02$ pF.

B. 35 GHz Rectenna Implemented with a Microstrip Patch Antenna

Fig. 14 shows a 35 GHz rectenna incorporating a patch antenna. The size and input impedance of the square patch antenna were calculated to be 2.6 mm^2 and 220 Ω using the cavity model [14]. The circuit was etched on a RT/duroid substrate with a thickness of 10 mil and a dielectric constant of 2.2. The matching network between the antenna and the diode was designed to provide a 40 Ω impedance at the fundamental frequency and a −j87 Ω impedance at the second harmonic to the diode. The matching network is realized with a single stub. The dimensions of the matching network were determined to be $L_1 = 2.39$ mm, $L_2 = 1.16$ mm, $W_1 = 0.35$ mm, $L_3 = 0.81$ mm, $W_2 = 0.1$ mm and $S = 0.5$ mm. One terminal of the diode was connected to the ground plane via a hole. The dc output line was connected to the center of the nonradiating edge of the patch antenna.

The power conversion efficiencies were measured using a waveguide array simulator shown in Fig. 15 to simulate the array environment. The rectenna was attached to the waveguide section that expanded the cross section area of a *Ka*-band waveguide (WR-28). Fig. 16 shows the measured efficiency with a 100 Ω load resistance. The maxi-

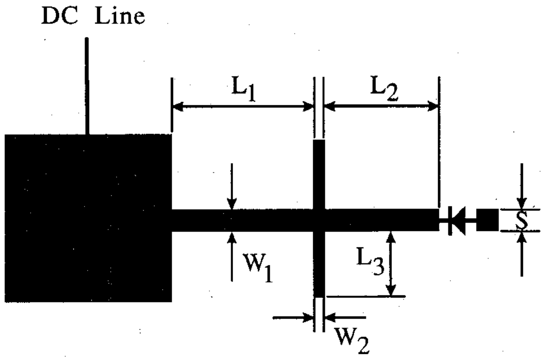

Fig. 14. 35 GHz rectenna using a patch antenna.

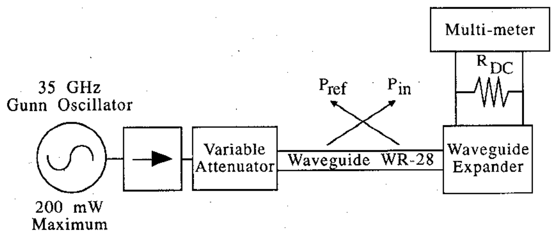

Fig. 15. Waveguide array simulator setup for the measurement of the 35 GHz to DC power conversion efficiency.

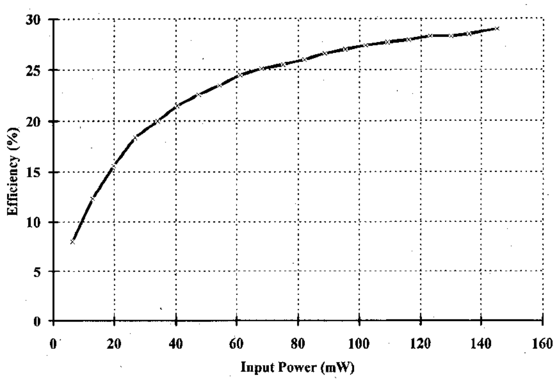

Fig. 16. The power conversion efficiency of the 35 GHz rectenna measured with the waveguide array simulator.

mum conversion efficiency measured with the patch rectenna was 29% at an net input power of 120 mW.

V. Frequency Selective Surface

The radiation of harmonics has been identified as a potential problem for land-based and space-based rectennas. For large rectenna arrays, these harmonics could radiate freely into the surrounding environment at significant power levels to interfere with communications or harm the immediate inhabitants. Frequency selective surfaces (FSSs) have long been recognized for their filtering characteristics. Because the second harmonic power level is on a level of 20 dB larger than the higher order harmonics on a resistively loaded rectenna [10], an attempt is made to reduce the level of its radiation while totally transmitting the fundamental frequency.

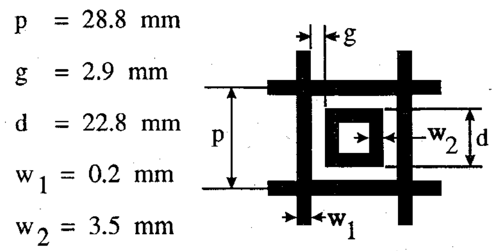

Fig. 17. Dimensions of the unit cell for the gridded square frequency selective surface.

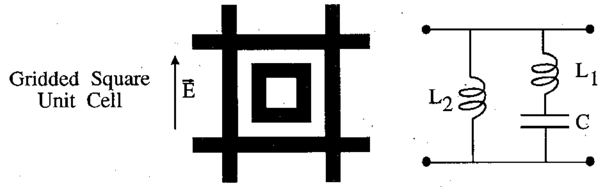

Fig. 18. Equivalent circuit for the gridded square FSS element.

The format of the FSS is a gridded square array and a unit cell of the gridded square is shown in Fig. 17. The equivalent circuit is shown in Fig. 18. For a vertically incident electric field, an inductance L_2 represents the grid and a series resonant inductance L_1 and capacitance C represent the squares.

The equations given below are used to design for the transmission and rejection bands [15]. Solving for the circuit admittance, the transmission coefficient is given by

$$|T|^2 = \frac{4}{4 + |Y|^2}$$

where

$$Y = \frac{X_1 + X_2 - \frac{1}{B}}{X_2\left(X_1 - \frac{1}{B}\right)}$$

The values of L_1, L_2 and C are given as

$$X_1 = \omega L_1 = 2(X_2 \| X_3)$$

$$X_2 = \omega L_2 = F(p, w_1, \lambda)$$

$$B = \omega C = 2\epsilon_r F(p, g, \lambda) \cdot \frac{d}{p}$$

where

$$X_3 = F(p, 2w_2, \lambda) \cdot \frac{d}{p}$$

where p, g, d, w_1 and w_2 are the dimensions defined in Fig. 17.

The immittances can be solved for TE- and TM-incidence at oblique angles. In this application, the incident angle is assumed normal to the array plane. The resulting

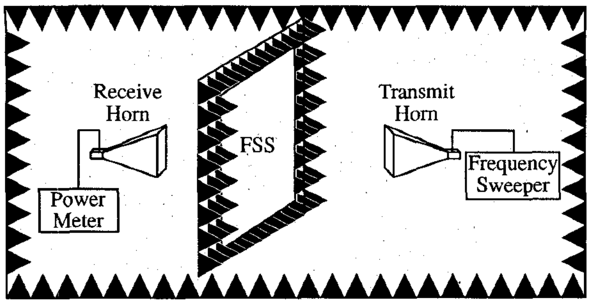

Fig. 19. FSS measurement setup in the anechoic chamber.

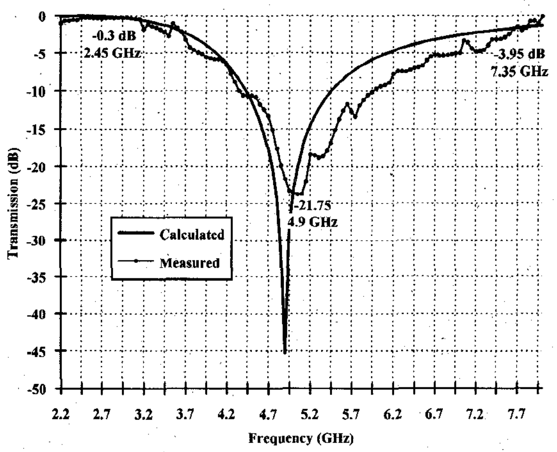

Fig. 20. Calculated and measured frequency response of the gridded square FSS array. The dimensions are: $p = 28.8$ mm, $g = 2.9$ mm, $d = 22.8$ mm, $w_1 = 0.2$ mm, and $w_2 = 3.5$ mm.

equations are then formed as

$$F(p, w, \lambda) = \frac{p}{\lambda}\left[\ln csc\left(\frac{\pi w}{2p}\right) + G(p, w, \lambda, \theta \,\&\, \phi = 0°)\right]$$

$$F(p, g, \lambda) = \frac{p}{\lambda}\left[\ln csc\left(\frac{\pi g}{2p}\right) + G(p, g, \lambda, \theta \,\&\, \phi = 0°)\right]$$

where G is a correction term [15].

The design calls for complete transmission at 2.45 GHz and reflection at 4.9 GHz. Using Microsoft Excel's spreadsheet, the dimensions of the gridded square shown in Fig. 17 were determined by the solver command. The equivalent circuit formulas require the substrate to be electrically thin. Therefore, Kapton F film ($\epsilon_r = 3.8$) that is 1 mil thick with 1 oz copper laminated on one side of the sheet was selected. Due to the small thickness of the substrate, the effective dielectric constant used for the design was 1.

The FSS was tested in an anechoic chamber similarly to the method in [16]. The FSS was taped onto a low density Styrofoam panel. It was then mounted and tested in the chamber as shown in Fig. 19. The frame holding the FSS was covered by absorbers to eliminate edge diffraction. The filtering response of the FSS was tested by comparing the difference in power at the receiver horn with and without the FSS when varying the frequency from 2.2 GHz to 8 GHz in 50 MHz steps.

The theoretical and measured response of the FSS are shown in Fig. 20. The agreement is fairly good. Over 20 dB rejection is achieved for the second harmonic of 4.9 GHz. The insertion loss at 2.45 GHz is 0.3 dB.

The FSS was next tested with a small 18" × 18" rectenna array. The FSS was spaced a $\lambda/4$ wavelength (3.06 cm) in front of the rectenna and illuminated at normal incidence. The gap on the perimeter between the FSS and rectenna plane was enclosed with metal to prevent power from radiating out the sides. The radiation peaks in the measured pattern of the second harmonic (4.9 GHz) with the FSS attached were decreased approximately 10 dB compared to the measured pattern without the FSS. The conversion efficiency of the rectenna decreased by less than 1% when the FSS was added.

VI. Conclusions

A microstrip measurement system has been developed to analyze packaged GaAs Schottky barrier diodes under small and large signal conditions. A computer program was written to analyze a rectenna circuit and calculate the conversion efficiency. The small signal diode equivalent circuit was implemented in the program and successfully related to the experimental results at 2.45 GHz. The maximum theoretical efficiency was calculated as 91% and the maximum measured efficiency was 85% when operating at an input power level of 1.2 watts. A 35 GHz rectenna was designed based on the computer analysis. The rectenna was built using a microstrip patch antenna and *Ka*-band mixer diode. The measured efficiency was 29% at 120 mW input power. A frequency selective surface was designed using an equivalent circuit model and tested to pass 2.45 GHz and reject the second harmonic of 4.9 GHz. Approximately 10 dB of attenuation occurred at 4.9 GHz on a small rectenna array and the conversion efficiency decreased by less than 1%. These results should be useful for future microwave power transmission system designs.

Acknowledgment

The advice, assistance, and encouragement given by W. C. Brown, R. M. Dickinson, and Dr. A. D. Patton are acknowledged. The loan agreement between the Jet Propulsion Laboratory and Texas A&M for the GaAs diodes is also acknowledged.

References

[1] W. C. Brown, "The history of power transmission by radio waves," *IEEE Trans. Microwave Theory Tech.*, vol. MTT-32, no. 9, pp. 1230–1242, Sept. 1984.

[2] ——, "The history of the development of the rectenna," in *Proc. Space Power Symp.*, 1980, pp. 271–280.
[3] ——, "Progress in the efficiency of free-space microwave power transmission," *J. Microwave Power*, vol. 7, no. 3, pp. 223–230, 1972.
[4] ——, "Electronic and mechanical improvement of the receiving terminal of a free-space microwave power transmission system," Raytheon Company, Wayland, MA, Tech. Report PT-4964, NASA Report No. CR-135194, NASA Contract No. NAS 3-19722, Aug. 1977.
[5] "Reception-conversion subsystem (RXCV) for microwave power transmission system final report," Raytheon Co., Sudbury, MA, Tech. Report No. ER75-4386, JPL Contract No. 953968, NASA Contract No. NAS 7-100, Sept. 1975.
[6] J. O. McSpadden, T. Yoo, and K. Chang, "Diode characterization in a microstrip measurement system for high power microwave power transmission," in *1992 IEEE MTT-S Int. Microwave Symposium Dig.*, 1992, pp. 1015–1018.
[7] P. T. Greiling and R. W. Laton, "Determination of semiconductor junction device package networks," *IEEE Trans. Microwave Theory Tech.*, vol. MTT-22, no. 12, pp. 1140–1145, Dec. 1974.
[8] D. N. Held and A. R. Kerr, "Conversion loss and noise of microwave and millimeterwave mixer: Part 1—Theory," *IEEE Trans. Microwave Theory Tech.*, vol. MTT-26, no. 2, pp. 44–55, Feb. 1978.
[9] T. Yoo, J. O. McSpadden, and K. Chang, "35 GHz rectenna implemented with a patch and a microstrip dipole antenna," in *1992 IEEE MTT-S Int. Microwave Symposium Dig.*, 1992, pp. 345–348.
[10] R. M. Dickinson, "Beamed microwave power transmitting and receiving subsystems radiation characteristics," Jet Propulsion Laboratory, California Institute of Technology, Pasadena, Publication 80-11, June 1980.
[11] J. O. McSpadden and K. Chang, "Suppression of rectenna harmonic radiation by a frequency selective surface," presented at *1992 IEEE-APS/URSI/NEM Joint Symposia*, Chicago, 1992.
[12] W. C. Brown, "Free-space microwave power transmission study, combined phase III and final report," Raytheon Co., Waltham, MA, Tech. Report No. PT-4601, NASA Contract No. NAS-8-25374, pp. 5-23–5-46, Sept. 1975.
[13] W. C. Brown, "Design definition of a microwave power reception and conversion system for use on a high altitude powered platform," Raytheon Co., Wallops Flight Facility, VA, NASA Report No. CR-156866, NASA Contract No. NAS 6-3006, July 1980.
[14] K. R. Carver and J. W. Mink, "Microstrip antenna technology," *IEEE Trans. Antennas Propagat.*, vol. AP-29, pp. 2–24, Jan. 1981.
[15] C. K. Lee and R. J. Langley, "Equivalent-circuit models for frequency-selective surfaces at oblique angles of incidence," *IEE Proc.*, vol. 132, Pt. H, No. 6, Oct. 1985.
[16] T. Cwik, R. Mittra, K. C. Lang, and T. K. Wu, "Frequency selective screens," *IEEE Antennas Propagation Society Newsletter*, Feature Article, pp. 6–10, Apr. 1987.

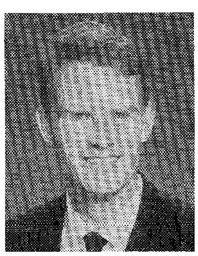

James O. McSpadden was born on June 26, 1966 in Denton, Texas. He received the B.S.E.E. degree from Texas A&M University in 1989.

From June 1989 to August 1990, he worked for Marathon Pipe Line Company in Houston as an Associate Engineer. At Marathon, he worked on cathodic protection projects and budget coordination. Presently at Texas A&M, he has been a Teaching Assistant and Research Assistant. As a Research Assistant, he has been involved with the Space Power project. His current research interests include rectenna arrays, frequency selective surfaces and quasi-optical power combining. He is pursuing a M.S.E.E. degree under Dr. Kai Chang and is a member of Eta Kappa Nu and Tau Beta Pi.

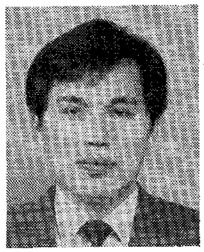

Taewhan Yoo received the B.S. degree in nuclear engineering from Seoul National University at Seoul, Korea in 1981, the M.S. degree in physics from Korea Advanced Institute of Science and Technology at Seoul, Korea in 1983.

From 1983 to 1988 he was with Electronics and Telecommunication Research Institute at Taejon, Korea. His research area was the development of opto-electronic devices for fiber optic communication. He is currently working on his doctoral dissertation at Texas A&M University, College Station, on microwave power transmission. His interests include microwave integrated circuit and its CAD design, wireless communication, and optoelectronic devices.

Kai Chang (S'75–M'76–SM'76–F'91) received the B.S.E.E. degree from the National Taiwan University, Taipei, Taiwan; the M.S. degree from the State University of New York at Stony Brook; and the Ph.D. degree from the University of Michigan, Ann Arbor, in 1970, 1972, and 1976, respectively.

From 1972 to 1976, he worked for the Microwave Solid-State Circuits Group, Cooley Electronics Laboratory of the University of Michigan as a Research Assistant. From 1976 to 1978, he was employed by Shared Applications, Inc., Ann Arbor, where he worked in computer simulation of microwave circuits and microwave tubes. From 1978 to 1981, he worked for the Electron Dynamics Division, Hughes Aircraft Company, Torrance, CA, where he was involved in the research and development of millimeter-wave solid-state devices and circuits, power combiners, oscillators and transmittters. From 1981 to 1985, he worked for the TRW Electronics and Defense, Redondo Beach, CA, as a Section Head, developing state-of-the-art millimeter-wave integrated circuits and subsystems including mixers, VCO's, transmitters, amplifiers, modulators, upconverters, switches, multipliers, receivers, and transceivers. He joined the Electrical Engineering Department of Texas A&M University in August 1985 as an Associate Professor and was promoted to a Professor in 1988. In January 1990, he was appointed E-System Endowed Professor of Electrical Engineering. His current interests are in microwave and millimeter-wave devices and circuits, microwave integrated circuits, microwave optical interactions, and antennas.

Dr. Chang served as the editor of the four-volume *Handbook of Microwave and Optical Components* published by John Wiley & Sons, Inc. in 1989 and 1990. He is the editor of the *Microwave and Optical Technology Letters* and the *Wiley Book Series in Microwave and Optical Engineering*. He has published over 180 technical papers and several book chapters in the areas of microwave and millimeter-wave devices and circuits. He received the Special Achievement Award from TRW in 1984, the Halliburton Professor Award in 1988, the Distinguished Teaching Award in 1989, and the Distinguished Research Award in 1992 from the Texas A&M University.